Journal of Hazardous Materials 201–202 (2012) 155–161

Contents lists available at SciVerse ScienceDirect

Journal of Hazardous Materials

journal homepage: www.elsevier.com/locate/jhazmat

An inorganic–organic hybrid optical sensor for heavy metal ion detection based on immobilizing 4-(2-pyridylazo)-resorcinol on functionalized HMS

Tongge Liu, Gang Li*, Na Zhang, Yongying Chen

State Key Laboratory of Fine Chemicals, College of Chemical Engineering, Dalian University of Technology, Dalian, 116024, PR China

ARTICLE INFO

Article history:
Received 28 March 2011
Received in revised form
16 November 2011
Accepted 17 November 2011
Available online 29 November 2011

Keywords:
Optical sensor
HMS
Heavy metal ions
4-(2-Pyridylazo)-resorcinol

ABSTRACT

A novel and low-cost optical sensor for heavy metal ion detection has been prepared by immobilizing 4-(2-pyridylazo)-resorcinol (PAR) on the functionalized hexagonal mesoporous silica (HMS) via N-trimethoxysilylpropyl-N,N,N-trimethylammonium chloride (TMAC). The successful fabrication of this optical sensor is confirmed by extensive characterizations using FT-IR, low angle X-ray diffraction (XRD), UV–vis spectroscopy and N_2 sorption, meanwhile its colorimetric properties, selectivity, sensitivity and reversibility are also investigated. The optical sensor responds selectively to heavy metal ions, such as Fe^{3+}, Cd^{2+}, Ni^{2+}, Zn^{2+}, Pb^{2+}, Co^{2+}, Hg^{2+} and Cu^{2+} with a color change from yellow to orange or purple in alkaline solutions, while it shows a color change only for Cu^{2+} under strongly acidic conditions. At pH 12.0, this optical sensor has a high sensitivity that makes it possible to detect Cu^{2+} in aqueous solution with the detection limit as low as 40 ppb by naked-eye. This optical sensor also shows excellent reversibility and regeneration by treatment with a solution of EDTA.

1. Introduction

To detect and control heavy metal ions in aqueous solution is very important. The principal detection methods for heavy metal ions are atomic absorption or atomic emission spectroscopy (AAS/AES) and inductively coupled plasma mass spectrometry (ICPMS). These methods are costly, need sophisticated equipments and require extreme control of experimental procedures. Hence, during the last decade, there has been growing interest in the development of optical sensors which allow on-site, real-time qualitative or semiquantitative detection. These heavy metal ion sensors based on cellulose supported platforms [1], polyvinylchloride (PVC) [2], ethyl cellulose (EC) [2], membrane [3] or other polymers [4] are inexpensive, selective and reusable, but they show a limited sensitivity for detection below the permissible level of metal ions.

With recent advances in materials science and nanotechnologies, the development of the mesoporous materials as hosts is key to designing highly sensitive and selective optical sensors [5,6]. In recent years, the mesoporous materials such as MCM-41 and SBA-15 have been given much attention for the development of optical chemical sensors [7–14] due to their high surface areas, large pore diameters and uniform pore size. In this paper, we report the use of hexagonal mesoporous silica (HMS), another kind of mesoporous material, as solid supports to synthesize an inorganic–organic hybrid optical sensor. HMS mesoporous silica was first introduced by Pinnavaia and co-workers [15,16]. Compared with MCM-41 and SBA-15, HMS has a worm-like pore structure, thick pore walls and a high degree of condensation, therefore, it has higher thermal stability and high adsorption capacity.

A low-cost and commonly employed indicator is 4-(2-pyridylazo)-resorcinol (PAR), a highly sensitive and non-selective reagent applicable for many heavy metal ions. Its color changes from yellow to red when complexed with metal ions such as Co^{2+}, Zn^{2+}, Cd^{2+}, Ni^{2+}, Hg^{2+}, Pb^{2+} and Cu^{2+}. Some applications for PAR and its analogues have been put into practice [17–19]. In this article, a new heavy metal ions responsive optical sensor (HMS-TMAC-PAR) is prepared via grafted surface functionalization of the original HMS with N-trimethoxysilylpropyl-N,N,N-trimethylammonium chloride (TMAC) and then by immobilization of PAR probe. HMS-TMAC-PAR has some important advantages as a solid-state colorimetric sensor. Firstly, it can be used for naked-eye colorimetric detection of low concentrations of heavy metal ions. Secondly, at a specific pH, it shows a high selectivity and sensitivity for ultra-trace levels of Cu^{2+} in aqueous solution. Thirdly, it also has excellent reusability when detecting Cu^{2+} in aqueous solution.

2. Experimental

2.1. Reagents

Tetraethylorthosilicate (TEOS) was purchased from Tianjin Kermel Chemical Co., China. Dodecylamine (DDA) and nitric acid salts

* Corresponding author. Tel.: +86 411 8498 6113; fax: +86 411 8498 6113.
E-mail address: liganghg@dlut.edu.cn (G. Li).

0304-3894/$ – see front matter © 2011 Elsevier B.V. All rights reserved.
doi:10.1016/j.jhazmat.2011.11.060

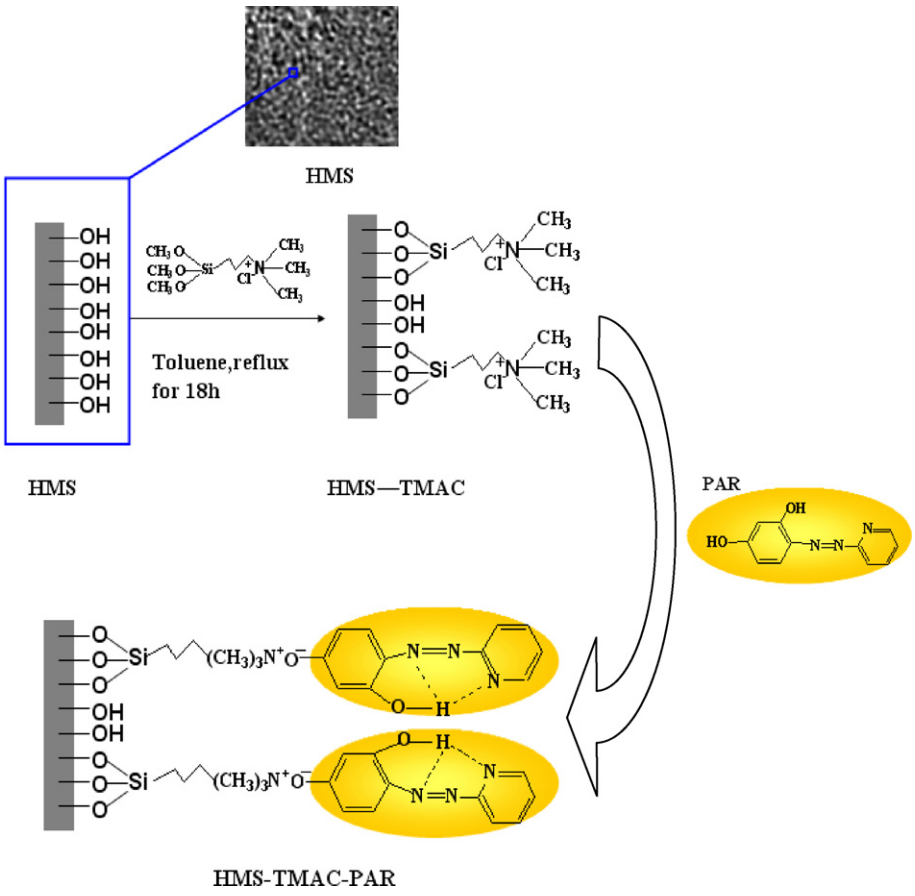

Scheme 1. Synthetic routes of HMS-TMAC and HMS-TMAC-PAR.

of various metals were obtained from Sinopharm Chemical Reagent Co., China. TMAC (50% methanol solution) was purchased from ABCR, Germany. PAR was purchased from Alfa Aesar China (Tianjin) Co., Ltd. All materials were of analytical reagent (AR) grade and used without further purification.

2.2. Apparatus and instruments

XRD patterns were recorded on a Rigaku D/Max-2400 diffractometer using Cu Kα radiation over the range of 0.5–10°. FT-IR spectra were recorded on a Bruker EQUINOX55 spectrometer, using KBr pellet technique. The thermogravimetric analysis (TGA) was performed with a Mettler Toledo TGA/SDTA851e. The elemental analysis was performed on an Elementar vario EL. The N_2 adsorption–desorption isotherms were measured using Quantachrome company AUTOSORB-1 physical adsorption apparatus at 77 K. Before the N_2 isothermal analysis, all samples were pretreated at 180 °C for 10 h. Specific surface area (S_{BET}) was calculated by using multipoint adsorption data from the linear portion of the N_2 adsorption isotherms based on the Brunauer–Emmett–Teller (BET) theory. The pore size distribution was then determined from the adsorption curve of the isotherms by using nonlocal density functional theory (NLDFT). The diffuse reflectance spectra of the sensor materials were recorded on a Jasco UV-500 spectrophotometer. A PHS-3C digital pH meter with a glass electrode was used to measure the pH value.

2.3. Synthesis of HMS

Synthesis of HMS was performed by dissolving DDA (2.0 g) in a mixed solvent of ethanol (19.0 mL) and water (28.0 mL), followed by the addition of TEOS (11.2 mL). The pH value of the mixture was adjusted to 9–11 with HCl. The final gel with a composition of molar ratio SiO_2:DDA:EtOH:HCl:H_2O = 1.0:0.27:6.5:0.02:36.5 was stirred constantly at room temperature for 18 h, and the resulting solid was collected by filtration, washed with abundant distilled water, dried at 100 °C and then calcined at 640 °C for 4 h to remove the organic template.

2.4. Fabrication of HMS-TMAC-PAR

With a grafting technique, HMS was first functionalized with TMAC by refluxing in toluene for 18 h under N_2 atmosphere. The functionalized HMS was washed thoroughly with ethanol and water to remove excess TMAC and then it was dried in an oven at 65 °C for 12 h to obtain HMS-TMAC. The immobilization of PAR on HMS-TMAC was performed by the addition of 0.6 g HMS-TMAC solid to PAR solution (9.3×10^{-5} M, 180 mL) under stirring for 3 h. The collected product was thoroughly washed with deionized water to remove excess PAR. The resulting HMS-TMAC-PAR was dried at 65 °C overnight and then ground to fine powder. The synthetic routes of HMS-TMAC and HMS-TMAC-PAR were illustrated in Scheme 1.

2.5. Colorimetric detection of metal ions

Concentration of stock solutions of the aqueous nitric acid salts (Al^{3+}, Mg^{2+}, Ca^{2+}, Na^{+}, Fe^{3+}, Cd^{2+}, Ni^{2+}, Zn^{2+}, Pb^{2+}, Co^{2+}, Hg^{2+} and Cu^{2+}) was 1.25×10^{-3} M. The suspension solutions of HMS-TMAC-PAR (0.5 g L^{-1}) were prepared in aqueous solution at various pH values, which were adjusted with 0.2 M NaOH or 0.2 M HCl. Each time a 2 mL suspension solution of HMS-TMAC-PAR was filled in a

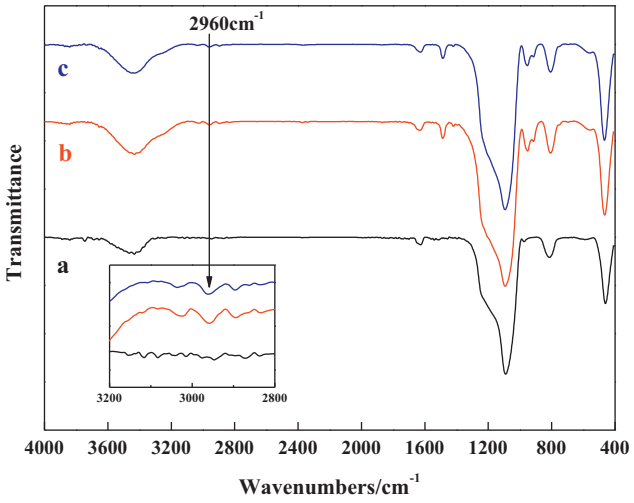

Fig. 1. FT-IR spectra of (a) HMS, (b) HMS-TMAC, and (c) HMS-TMAC-PAR.

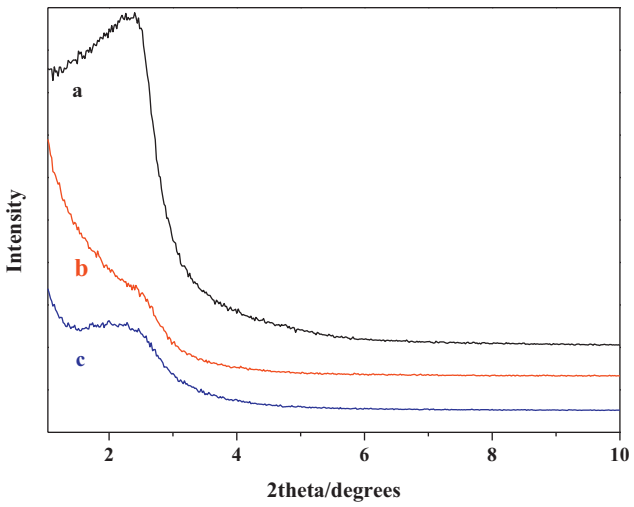

Fig. 2. Low-angle XRD patterns of (a) HMS, (b) HMS-TMAC, and (c) HMS-TMAC-PAR.

1 cm quartz cell and different stock solutions of cations were added into the quartz cell gradually by using a micro-syringe. The volume of added stock solution was less than 100 μL in order to keep the total volume of testing solution without obvious change. The heavy metal ions were estimated qualitatively using naked-eye colorimetric assessment and Cu^{2+} was detected quantitatively using UV–vis reflectance spectrometry at 510 nm.

3. Results and discussion

3.1. Characteristics of HMS-TMAC-PAR

FT-IR spectra of HMS, HMS-TMAC and HMS-TMAC-PAR are shown in Fig. 1. For all samples, the bands at 3438 and 1633 cm^{-1} are attributed to the stretching and bending vibrations of the surface silanol groups Si–OH, respectively. In addition, the typical Si–O–Si bands associated with the formation of a condensed silica network are present at 1095, 812 and 460 cm^{-1} [20]. However, HMS-TMAC and HMS-TMAC-PAR show additional absorption bands at 2960 and 1485 cm^{-1}, which are due to the aliphatic C–H and the stronger C–N bonds, respectively [21,22]. These results illustrate the mesoporous silica (HMS) is grafted by TMAC organic molecules.

The XRD patterns of HMS, HMS-TMAC and HMS-TMAC-PAR are given in Fig. 2. All of the patterns contain a single low-angle diffraction peak at about $2\theta = 2^{\circ}$, which represents a characteristic of the mesoporous silica (HMS). However, the intensities of the peak of sample (b) and (c) decrease, suggesting that the mesoporous structures of sample (b) and (c) become less uniform upon the introduction of the organic molecules into HMS.

The result of thermal analysis for HMS-TMAC sample is shown in Fig. 3. The TG profile shows two-step decrease in weight of HMS-TMAC. The total weight loss is about 16% between 170 and 750 °C. Two broad peaks are observed at 75 and 270 °C on DTG curve. The former can be due to the desorption of adsorbed H_2O on the surface of the mesoporous silica (HMS) [23] and the latter can be due to the decomposition of the TMAC fragments [6]. Table 1 shows the carbon and nitrogen contents of the functionalized HMS increase noticeably relative to the original HMS and the molar ratio of carbon to nitrogen close to 6 is consistent with the synthetic route of HMS-TMAC (Scheme 1). The thermal analysis result and the elemental analysis results demonstrate that the HMS support is successfully functionalized by TMAC organic molecules.

Table 1
Elemental analyses of HMS and HMS-TMAC.

Sample	N (wt%)	C (wt%)	H (wt%)
HMS	0.02	0.21	0.33
HMS-TMAC	1.51	9.40	2.56

Fig. 4 shows UV–vis diffuse reflectance spectra of HMS, HMS-TMAC, HMS-TMAC-PAR and solid PAR. In near ultraviolet region, it can be seen that a series of bands at 210, 260 and about 315 nm emerges in the spectra of HMS-TMAC-PAR and solid PAR. These bands can be attributed to the typical electronic transition of the aromatic ring. And in the visible region, solid PAR exhibits a strong absorption band at 500 nm. Compared with solid PAR, the absorption band of HMS-TMAC-PAR is blue shifted from 500 nm to 400 nm, while HMS and HMS-TMAC show no absorption. These observations imply the PAR probe molecules have been successfully immobilized on HMS-TMAC.

Nitrogen physisorption measurements of HMS and HMS-TMAC-PAR are shown in Fig. 5. The N_2 adsorption–desorption isotherms show that HMS and HMS-TMAC-PAR exhibit typical type-IV isotherms according to the IUPAC classification with a step at a relative pressure of 0.2–0.4. From HMS to HMS-TMAC-PAR, the slope at P/P_0 of 0.2–0.4 becomes less steep, which indicates the uniformity of the pore size of HMS-TMAC-PAR drops relative to HMS. This is consistent with the low-angle XRD result. HMS and HMS-TMAC-PAR both have the appreciable type H1 hysteresis loops

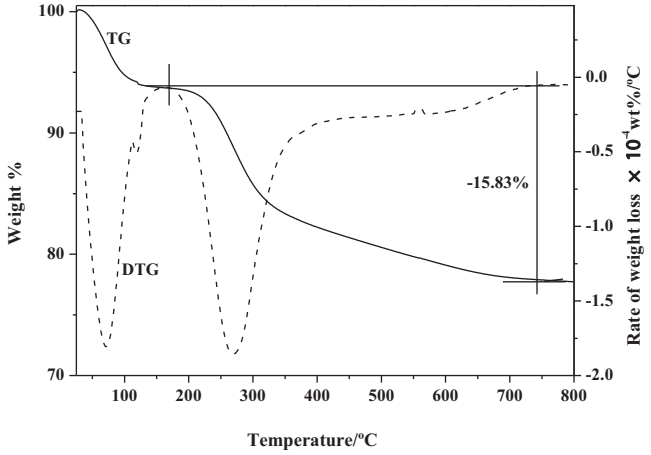

Fig. 3. TG and DTG curves of HMS-TMAC.

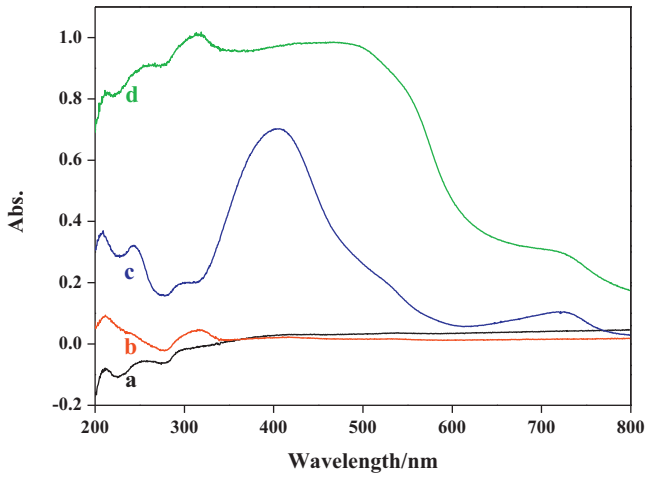

Fig. 4. UV–vis reflectance spectra of (a) HMS, (b) HMS-TMAC, (c) HMS-TMAC-PAR and (d) solid PAR.

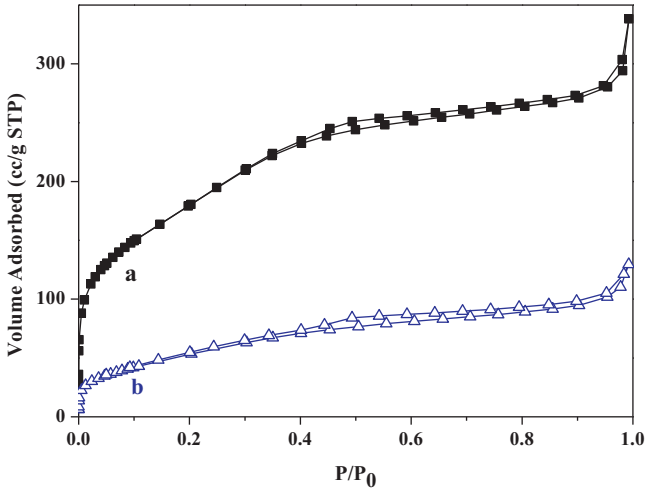

Fig. 5. N_2 adsorption–desorption isotherms of (a) HMS and (b) HMS-TMAC-PAR.

[24], indicating the presence of textural mesopores and cylindrical pores. But the hysteresis loop of HMS-TMAC-PAR emerges at lower relative pressure than that of HMS, which means the pores on the HMS-TMAC-PAR are smaller. The above phenomenon can also be proved by structural properties of HMS and HMS-TMAC-PAR. As shown in Table 2, the texture parameters of mesoporous silica HMS distinctly change after grafting the organic molecules. HMS-TMAC-PAR exhibits an increase in wall thickness and a considerable decrease in BET surface area, pore diameter and pore volume relative to HMS. These results also demonstrate that the organic molecules have grafted inside the mesopores.

3.2. HMS-TMAC-PAR responses to metal ions

After the addition of Al^{3+}, Mg^{2+}, Ca^{2+}, Na^{+}, Fe^{3+}, Cd^{2+}, Ni^{2+}, Zn^{2+}, Pb^{2+}, Co^{2+}, Hg^{2+} and Cu^{2+}, the color changes of HMS-TMAC-PAR (0.5 g L^{-1}, pH 9.0) aqueous suspension are shown in Fig. 6a and the color changes become more obvious after precipitating (Fig. 6b). More interestingly, heavy metal ions, such as Fe^{3+}, Cd^{2+}, Ni^{2+}, Zn^{2+}, Pb^{2+}, Co^{2+}, Hg^{2+} and Cu^{2+}, cause the color of HMS-TMAC-PAR changing from yellow to orange or purple. However, light metal ions, such as Al^{3+}, Mg^{2+}, Ca^{2+} and Na^{+}, fail to show any color change. It means that compared with PAR immobilized colorimetric fiber [25], HMS-TMAC-PAR can be used for naked-eye colorimetric detection of lower concentration of the heavy metal ions.

3.3. HMS-TMAC-PAR responses to Cu^{2+}

HMS-TMAC-PAR cannot only effectively distinguish between heavy metal ions and light metal ions through the color changes, but it has a high selectivity for low concentration of Cu^{2+} under strongly acidic conditions. The selectivity of HMS-TMAC-PAR is shown in Fig. 7. At pH 2.0, no color change is observed for other heavy metal ions, while only Cu^{2+} causes a color change from yellow to purple in the suspension of HMS-TMAC-PAR (0.5 g L^{-1}) (Fig. 7a). Fig. 7(b) shows that no significant effects on absorbance at $A_{510\,nm}/A_{420\,nm}$ with other heavy metal ions (such as Fe^{3+}, Cd^{2+}, Ni^{2+}, Zn^{2+}, Pb^{2+}, Co^{2+} and Hg^{2+}), but addition of Cu^{2+} results in a prominent enhancement of the absorbance at $A_{510\,nm}/A_{420\,nm}$. So HMS-TMAC-PAR has a high selectivity for detection of Cu^{2+} in strongly acidic solution.

Table 2
Structural properties of HMS and HMS-TMAC-PAR.

Sample	d_{100}[a] (nm)	a_0[b] (nm)	Pore diameter[c] (nm)	Wall thickness[d] (nm)	BET surface area (m^2/g)	Pore volume[e] (cm^3/g)
HMS	3.5	4.0	2.3	1.7	657	0.5
HMS-TMAC-PAR	3.9	4.5	1.8	2.7	202	0.2

[a] Calculated from XRD analysis.
[b] $a_0 = 2d_{100}/3^{1/2}$.
[c] Calculated from adsorption branch of nitrogen isotherm using BJH model.
[d] Wall thickness = a_0 − pore diameter.
[e] Calculated from the volume adsorbed of P/P_0 at 0.99.

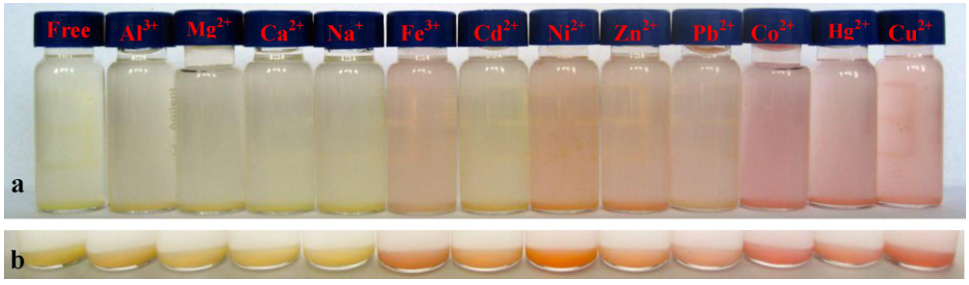

Fig. 6. Color changes of (a) the aqueous suspension of HMS-TMAC-PAR and (b) precipitated HMS-TMAC-PAR with different metal ions (6.25×10^{-6} M) at pH 9.0.

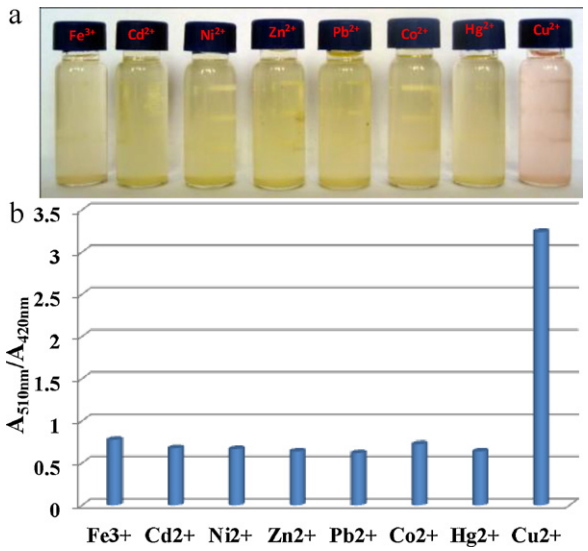

Fig. 7. Color changes (a) and the absorption response $A_{510\,nm}/A_{420\,nm}$ (b) of HMS-TMAC-PAR with different heavy metal ions (6.25×10^{-6} M) at pH 2.0.

Based on this property, the detection of Cu^{2+} in aqueous solution was systematically investigated as follows.

3.3.1. *Effect of pH on the detection of Cu^{2+}*

To explore the further utility of HMS-TMAC-PAR as a selective optical sensor for Cu^{2+} detection, the effect of pH was evaluated. The absorbance of HMS-TMAC-PAR without and with Cu^{2+} at different pH values are shown in Fig. 8. In a wide pH range, from 1 to 12, no obvious absorption of free HMS-TMAC-PAR is observed. However, in the presence of Cu^{2+}, the absorption intensity is gradually increasing in all pH range. These results show that the complexation between Cu^{2+} and the immobilized PAR is formed in a wide range of pH, from 1 to 14. Fig. 8 also shows that upon the addition of Cu^{2+}, the relative maximum absorption at pH 12.0, which is selected as the specific pH for detecting Cu^{2+} in aqueous solution using HMS-TMAC-PAR. So, we suggest that, for the sensitive detection of Cu^{2+} in the low concentration without any other heavy ions, pH 12.0 is selected. For the selective detection of Cu^{2+} in the presence of other heavy ions, pH 2.0 is selected.

3.3.2. *Spectrometer and naked-eye detection of Cu^{2+}*

Considering that the Environmental Protection Agency (EPA) standard for the maximum allowable level of Cu^{2+} is 1 ppm in drinking water, both the spectrometer and naked-eye detection limits of the HMS-TMAC-PAR for Cu^{2+} have been tested. For

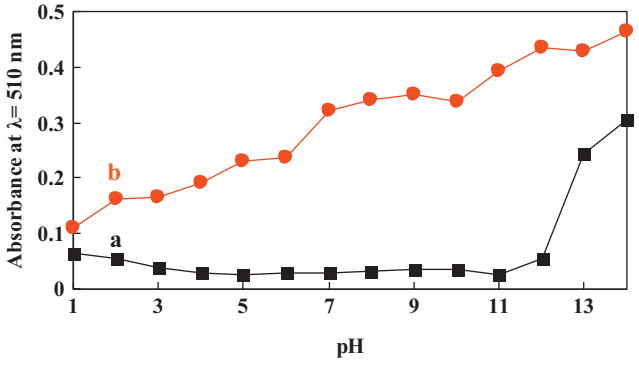

Fig. 8. Effect of pH on absorbance at 510 nm in UV–vis spectra of (a) free HMS-TMAC-PAR and (b) HMS-TMAC-PAR with the addition of Cu^{2+} (6.25×10^{-6} M).

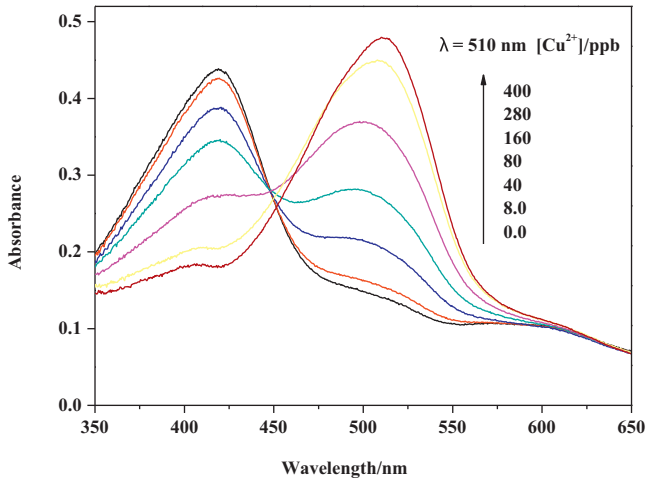

Fig. 9. UV–vis absorption spectra of HMS-TMAC-PAR with different concentrations of Cu^{2+} at pH 12.0.

spectrometer detection free HMS-TMAC-PAR in aqueous solution ($0.5\,g\,L^{-1}$) exhibits an absorption maximum at about 420 nm (pH 12.0). With the addition of Cu^{2+}, a new peak appears in the spectra of HMS-TMAC-PAR at 510 nm and the intensity of this peak becomes stronger (Fig. 9). These results indicate the formation of the complexation between Cu^{2+} and the immobilized PAR.

Fig. 10 represents the absorbance of HMS-TMAC-PAR at 510 nm against Cu^{2+} concentrations and shows a linear correlation in the range from 1.6 to 9.6 ppb with a correlation coefficient of 0.99 (Fig. 10, insert). The nonlinear nature of the curve at higher concentrations is due to saturation effects.

The spectrometer detection limit (D_L) of Cu^{2+} using the optical sensors is calculated from the data in the linear range of the calibration plot (Fig. 10, insert), according to the following Eq. (1) [26].

$$D_L = \frac{kS_b}{m} \quad (1)$$

where k is a factor equal to 3, S_b is the standard deviation of the blank and m is the slope of the calibration graph in the linear range (Fig. 10, insert). The calculated S_b is 0.076% after five successive measurements to assure the accuracy and precision of the detection method. The resultant D_L value is 0.81 ppb which demonstrates that the optical sensors can be used in quantitative analysis of the concentration of Cu^{2+} at the parts per billion levels at pH 12.

The naked-eye detection of Cu^{2+} is achieved at a concentration range of 40–400 ppb using HMS-TMAC-PAR. A significant color change for HMS-TMAC-PAR is observed from yellow to purple with an increase in Cu^{2+} concentration (Fig. 11). This also demonstrates

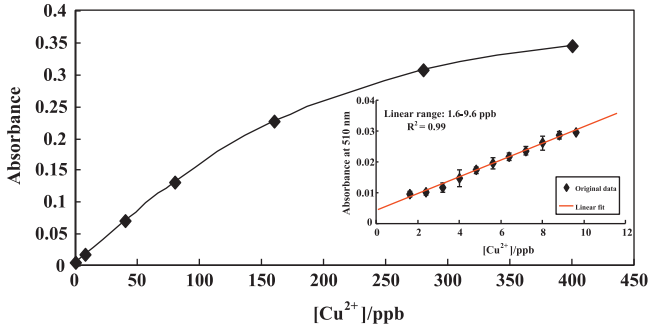

Fig. 10. Calibration curves of the absorbance of HMS-TMAC-PAR with different concentrations of Cu^{2+} at pH 12.0 at 510 nm.

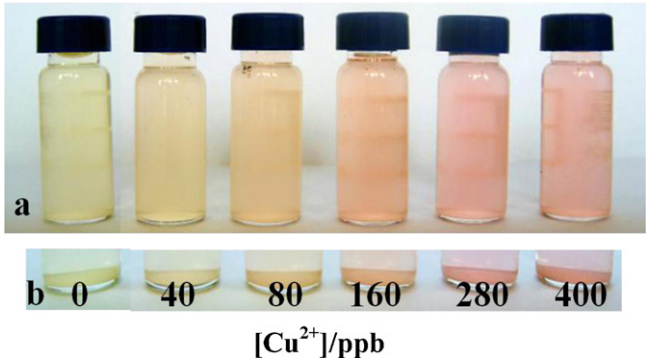

Fig. 11. Color changes of (a) the aqueous suspension of HMS-TMAC-PAR and (b) precipitated HMS-TMAC-PAR with different concentrations of Cu^{2+} at pH 12.0.

that HMS-TMAC-PAR can be used for the rapid detection of ultra-trace levels of Cu^{2+} by naked eye without any instrumentation.

The detection limits of HMS-TMAC-PAR for Cu^{2+} are 0.81 ppb by spectrometer and 40 ppb by naked-eye. That means the HMS-TMAC-PAR could detect Cu^{2+} under 1 ppm and accord with the EPA standard by both spectrometer and naked-eye.

3.3.3. Response time of HMS-TMAC-PAR

To obtain the response time of HMS-TMAC-PAR upon addition of Cu^{2+}, the absorbance at different time intervals was detected, as shown in Fig. 12. After addition of 6.25×10^{-6} M of Cu^{2+}, the absorbance increases quickly within 60 s and then remains constant with time, which shows that the reaction has completed. So HMS-TMAC-PAR can provide fast colorimetric detection.

3.3.4. Reversibility of HMS-TMAC-PAR

Reversibility and regeneration are the major advantages of the solid sensors in practical applications [27]. Fig. 13 illustrates the reversibility of HMS-TMAC-PAR. The color of free HMS-TMAC-PAR is yellow (Fig. 13, 1), while it changes from yellow to purple with the addition of Cu^{2+} (6.25×10^{-6} M, for example Fig. 13, 2). The addition of an aqueous solution of EDTA (7.5×10^{-6} M) to the suspension of HMS-TMAC-PAR-Cu^{2+} causes a color change from purple to yellow (for example Fig. 13, 3), which is due to the stability constant of Cu^{2+}-EDTA is larger than that of Cu^{2+}-PAR [28]. Subsequently, EDTA need not be separated from the system, and it is observed the color changes from yellow to purple again by addition of Cu^{2+} (for example Fig. 13, 4). This course can be repeated at least five times. So HMS-TMAC-PAR can be used repeatedly for the naked-eye detection of Cu^{2+} in aqueous solution.

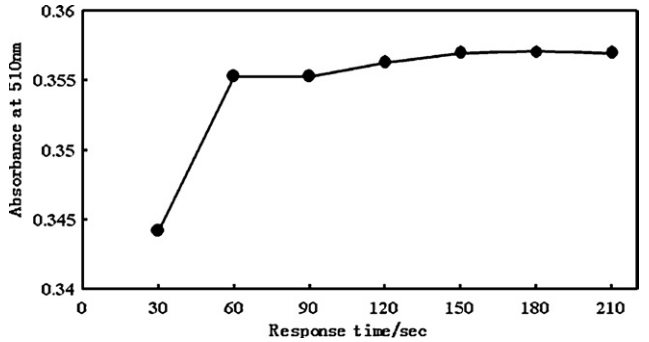

Fig. 12. Response time of HMS-TMAC-PAR (0.5 g L^{-1}, pH 12.0) with Cu^{2+} (6.25×10^{-6} M).

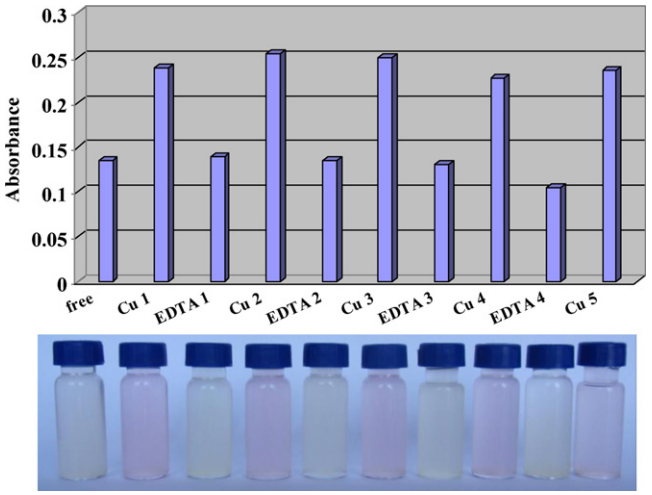

Fig. 13. UV–vis absorption spectra and color changes of HMS-TMAC-PAR with Cu^{2+} and EDTA.

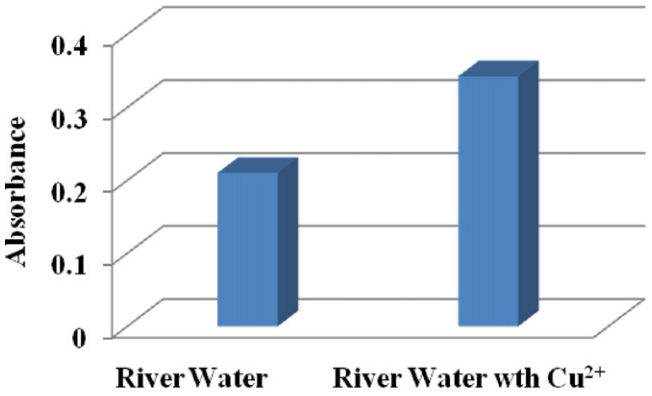

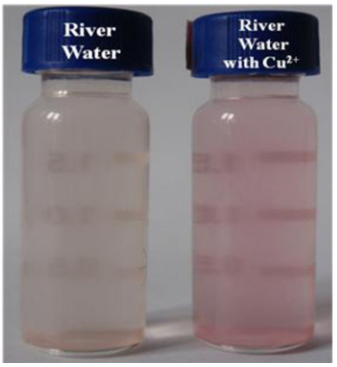

Fig. 14. Absorbance and color changes of HMS-TMAC-PAR in river water and river water with Cu^{2+} (6.25×10^{-6} M).

3.3.5. HMS-TMAC-PAR responses to Cu^{2+} in real sample

To evaluate whether HMS-TMAC-PAR can detect Cu^{2+} in environmental samples, a water sample collected from LingShui River in Dalian, China was used without any treatment (pH 8.42). With the addition of Cu^{2+} (6.25×10^{-6} M), a significant color change of HMS-TMAC-PAR from yellow to purple could be observed by naked-eye (as shown in Fig. 14). So HMS-TMAC-PAR is promised to be explored into a practical sensor.

4. Conclusions

HMS-TMAC-PAR used for naked-eye selective detection of heavy metal ions is designed by the immobilization of PAR on the

functionalized HMS. In alkaline solutions, HMS-TMAC-PAR could distinguish heavy metal ions from light metal ions by naked-eye colorimetric detection. While in acidic solutions (pH 2.0), HMS-TMAC-PAR responds selectively to Cu^{2+}, which makes it a useful specific monitor for Cu^{2+} in aqueous solution. In addition, at pH 12.0, HMS-TMAC-PAR has a high sensitivity for low concentration of Cu^{2+} and allows the naked-eye detection of Cu^{2+} as low as 40 ppb. In general, HMS-TMAC-PAR provides extraordinary sensitivity, reusability and fast colorimetric detection of heavy metal ions, especially Cu^{2+} for tracking of heavy metal pollutants in the environment. In the future research, we will focus on fabricating solid-state colorimetric sensors by immobilizing different probe molecules on HMS to detect various toxic ions in aqueous solution. This work will also expand the application of mesoporous silica HMS.

Acknowledgements

The authors are grateful for the financial support from Program for New Century Excellent Talents in University (NCET-04-0270), National Natural Science Foundation of China (no. 20406005) and Central University basic research fund (DUT10LK11).

References

[1] J.H. Poplin, R.P. Swatloski, J.D. Holbrey, S.K. Spear, A. Metlen, M. Gratzel, M.K. Nazeeruddin, R.D. Rogers, Sensor technologies based on a cellulose supported platform, Chem. Commun. 202 (2007) 5–2027.
[2] O. Oter, K. Ertekin, C. Kirilmis, M. Koca, Spectral characterization of a newly synthesized fluorescent semicarbazone derivative and its usage as a selective fiber optic sensor for copper(II), Anal. Chim. Acta 584 (2007) 308–314.
[3] Y. Kalyan, A.K. Pandey, P.R. Bhagat, R. Acharya, V. Natarajan, G.R.K. Naidu, A.V.R. Reddy, Membrane optode for mercury(II) determination in aqueous samples, J. Hazard. Mater. 166 (2009) 377–382.
[4] Y. Morishima, T. Sato, M. Kamachi, Spectroscopic studies of competitive binding of thallium and alkaline-earth metal cations onto poly(sodium acrylate-*co*-acrylamide) tagged with optical probes, Macromolecules 29 (1996) 3960–3964.
[5] S.A. El-Safty, D. Prabhakaran, A.A. Ismail, H. Matsunaga, F. Mizukami, Nanosensor design packages: a smart and compact development for metal ions sensing responses, Adv. Funct. Mater. 17 (2007) 3731–3745.
[6] S.A. El-Safty, A.A. Ismail, H. Matsunaga, F. Mizukami, Optical nanosensor design with uniform pore geometry and large particle morphology, Chem. Eur. J. 13 (2007) 9245–9255.
[7] M. Wark, Y. Rohlfing, Y. Altindag, H. Wellmann, Optical gas sensing by semiconductor nanoparticles or organic dye molecules hosted in the pores of mesoporous siliceous MCM-41, Phys. Chem. Chem. Phys. 5 (2003) 5188–5194.
[8] S. Basurto, T. Torroba, M. Comes, R. Martinez-Manez, F. Sancenon, L. Villaescusa, P. Amoros, New chromogenic probes into nanoscopic pockets in enhanced sensing protocols for amines in aueous environments, Org. Lett. 7 (2005) 5469–5472.
[9] K. Kledzik, M. Orlowska, D. Patralska, M. Gwiazda, J. Jezierska, S. Pikus, R. Ostaszewski, A.M. Kłonkowski, Cu(II) recognition materials: fluorophores grafted on mesoporous silica supports, Appl. Surf. Sci. 254 (2007) 441–451.
[10] M. Comes, M.D. Marcos, R. Martinez-Manez, F. Sancenon, L.A. Villaescusa, A. Graefe, G.J. Mohr, Hybrid functionalised mesoporous silica-polymer composites for enhanced analyte monitoring using optical sensors, J. Mater. Chem. 18 (2008) 5815–5823.
[11] R. Metivier, I. Leray, B. Lebeau, B. Valeur, A mesoporous silica functionalized by a covalently bound calixarene-based fluoroionophore for selective optical sensing of mercury(II) in water, J. Mater. Chem. 15 (2005) 2965–2973.
[12] E. Kim, H.E. Kim, S.J. Lee, S.S. Lee, M.L. Seo, J.H. Jung, Reversible solid optical sensor based on acyclic-type receptor immobilized SBA-15 for the highly selective detection and separation of Hg(II) ion in aqueous media, Chem. Commun. 33 (2008) 3921–3923.
[13] L.L. Li, H. Sun, C.J. Fang, J. Xu, J.Y. Jin, C.H. Yan, Optical sensors based on functionalized mesoporous silica SBA-15 for the detection of multianalytes (H^+ and Cu^{2+}) in water, J. Mater. Chem. 17 (2007) 4492–4498.
[14] X.Y. Wang, P. Wang, Z.H. Dong, Z.P. Dong, Z.Y. Ma, J. Jiang, R. Li, J.T. Ma, Highly sensitive fluorescence probe based on functional SBA-15 for selective detection of Hg^{2+}, Nanoscale Res. Lett. 5 (2010) 1468–1473.
[15] P.T. Tanev, M. Chibwe, T.J. Pinnavaia, Titanium-containing mesoporous molecular sieves for catalytic oxidation of aromatic compounds, Nature 368 (1994) 321–323.
[16] P.T. Tanev, T.J. Pinnavaia, A neutral templating route to mesoporous molecular sieves, Science 267 (1995) 865–867.
[17] C.E. Sabel, J.L. Shepherd, S. Siemann, A direct spectrophotometric method for the simultaneous determination of zinc and cobalt in metalloproteins using 4-(2-pyridylazo)resorcinol, Anal. Biochem. 391 (2009) 74–76.
[18] E. Engstrom, I. Jonebring, B. Karlberg, Assessment of a screening method for metals in seawater based on the non-selective reagent 4-(2-pyridylazo)resorcinol (PAR), Anal. Chim. Acta 371 (1998) 227–234.
[19] I.V. Vyshcherevich, I.E. Kalinichenko, Photometric determination in drinking water of cobalt and nickel with 4-(2-pyridylazo)resorcinol, J. Water Chem. Technol. 32 (2010) 33–38.
[20] C. Chen, L.P Zhou, Q.H Zhang, H. Ma, H. Miao, J. Xu, Design of bifunctionalized hexagonal mesoporous silicas for selective oxidation of cyclohexane, Nanotechnology 18 (2007) 215603.
[21] Q. Wei, Z.R. Nie, Y.L. Hao, L. Liu, Z.X. Chen, J.X. Zou, Effect of synthesis conditions on the mesoscopical order of mesoporous silica SBA-15 functionalized by amino groups, J. Sol-Gel Sci. Technol. 39 (2006) 103–109.
[22] Z. Yan, G.T. Li, L. Mu, S.Y. Tao, Pyridine-functionalized mesoporous silica as an efficient adsorbent for the removal of acid dyestuffs, J. Mater. Chem. 16 (2006) 1717–1725.
[23] H.G. Chen, J.L. Shi, H.R. Chen, Y.S. Li, Z.L. Hua, D.S. Yan, Strong visible photoluminescence of TEEDPS-modified silica MCM-41 materials, Appl. Phys. B 77 (2003) 89–91.
[24] K.S.W. Sing, D.H. Everett, R.A.W. Haul, L. Moscow, R.A. Pierotti, J. Rouquerol, T. Siemieniewska, Reporting physisorption data for gas/solid systems with special reference to the determination of surface area and porosity, Pure Appl. Chem. 57 (1985) 603–619.
[25] G.W. Li, L.H. Zhang, Z.W. Li, W.Q. Zhang, PAR immobilized colorimetric fiber for heavy metal ion detection and adsorption, J. Hazard. Mater. 177 (2010) 983–989.
[26] S.A. El-Safty, A.A. Ismail, H. Matsunaga, H. Nanjo, F. Mizukami, Uniformly mesocaged cubic *Fd*3*m* monoliths as modal carriers for optical chemosensors, J. Phys. Chem. C 112 (2008) 4825–4835.
[27] A.A. Ismail, A selective optical sensor for antimony based on hexagonal mesoporous structures, J. Colloid Interface Sci. 317 (2008) 288–297.
[28] M. Zenki, Y. Iwadou, T. Yokoyama, Flow-injection analysis of copper(II) with PAR in the presence of EDTA, Anal. Sci. 18 (2002) 1077–1079.